Optik - International Journal for Light and Electron Optics 287 (2023) 171118

Contents lists available at ScienceDirect

Optik - International Journal for Light and Electron Optics

journal homepage: www.elsevier.com/locate/ijleo

Original research article

Detailed analysis for temperature-dependent and temperature-independent Goos–Hänchen shift

Aniqa Mehboob [a,b,*], Fabio Mangini [a,c], Fabrizio Frezza [a,c]

[a] Department of Information Engineering, Electronics and Telecommunications, Sapienza University of Rome, Via Eudossiana 18, 00184, Rome, Italy

[b] Department of Basic and Applied Sciences for Engineering, Sapienza University of Rome, 00185, Rome, Italy

[c] CNIT: National, Inter-University Consortium for Telecommunications, Viale G.P. Usberti, 181/A, 43124 Parma, Italy

ARTICLE INFO

Keywords:
Temperature-dependent Goos–Hänchen shift
Drude's model
Reflectivity
Dielectric function

ABSTRACT

In this work, we have presented the deep insight of Goos–Hänchen shift depending upon the temperature when a plane incident electromagnetic beam of light enters from a rare to a denser medium, keeping conditions of total internal reflection intact. A simple well known Drude's model has been used for the purpose of thermal analysis of this shift. Through this model, the temperature-dependent permittivity of absorbing or complex medium has been found through the temperature-dependent plasma and damping wavelengths. Both transverse electric and magnetic incident electromagnetic fields have been considered in this regard. On an air–metal interface, firstly, Goos–Hänchen shift has been found when a temperature-independent dielectric function of a complex medium has been considered, and secondly, by analyzing the temperature-dependent dielectric function in the simplest way by using the stationary-phase method. This study is useful to understand the behavior of Goos–Hänchen shift around the temperature-dependency of the medium and how the angle of incidence impacts in this scenario.

1. Introduction

Generally, when a light beam incident on an interface which possesses different refractive indices, the beam bounces back at the same point as by the prediction of geometrical optics, but in 1947, it was observed that when the light beams that travel from media with different refractive indices deviate from the path of geometrical optics and travel a short distance along the interface. This optical phenomenon is referred to as lateral displacement or Goos–Hänchen shift (GH), and can be seen in Fig. 1(a,b) [1–4].

Mostly, this shift is mentioned under the situation of total internal reflection, when beams of light travel from optically sparse to a denser medium [5]. Artmann's work on the GH shift by using the stationary-phase method serves as a backbone for the theoretical interpretation [6]. Now it is more evident that deviating behavior of reflected rays exists and has been proved by considering a simple air-glass interface, shone by the Gaussian beam [7]. As Goos–Hänchen shift is a non-specular phenomenon and shows very interesting behavior for different media. The amplitude of this shift can be tuned as well, and many research groups are working on the electrically tunable GH-shift [8]. Temperature-dependent Goos–Hänchen shift is one step forward in this regard and has opened a new door in advanced optoelectronics, temperature-monitoring sensors and surface-plasmon resonance sensors [9,10]. Recently, plenty of literature has been developed, which leads to remarkable results ending with applications in optical switching and in sensing technology, including plasmon resonance sensors, oscillating wave-sensor and temperature-dependent sensors [9–11], lasers [12], and acoustic [13]. GH-shift also shows positive as well as negative behavior lean upon the media or refractive index

* Corresponding author.
E-mail address: aniqa.mehboob@uniroma1.it (A. Mehboob).

https://doi.org/10.1016/j.ijleo.2023.171118
Received 27 January 2023; Received in revised form 17 May 2023; Accepted 5 June 2023
Available online 4 July 2023

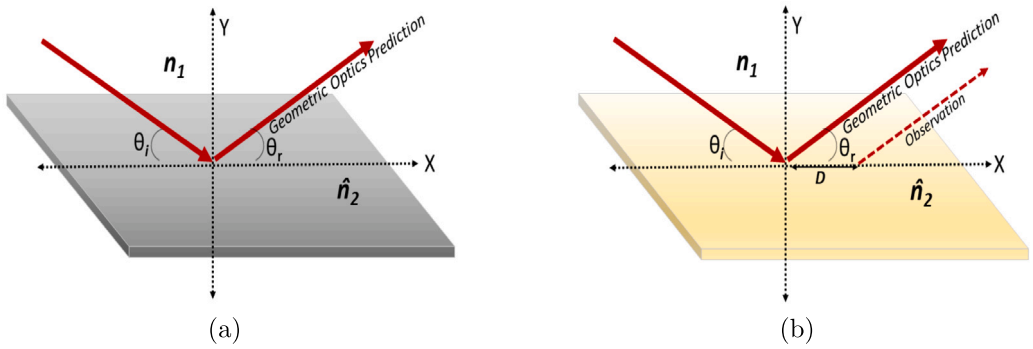

Fig. 1. Structural diagram for a planar interface. (a) Geometrical optics prediction for an incident beam at an interface; (b) observation of GH shift for an incident beam at a planar interface.

of media. Negative GH-shift has received considerable attention and has many applications in electromagnetic regime [14–16]. In recent studies, composite GH-shift has been explored, which is a combination of two shifts, when a Gaussian beam impinges on the interface and explains how the GH-shift changes its behavior for both s and p-polarization. Large positive and negative GH-shift has been observed when an incident beam hits on metal grating when the condition of surface plasmon resonance (SPR) has been satisfied. In these studies, it has been proved theoretically and experimentally as well that the incident beam width and grating depth influence the GH-shift [7,17–19]. In the recent past, a number of research groups have investigated the Goos–Hänchen shift in the context of temperature dependency while considering different media, including complex media [20,21], absorbing media [22,23], and metamaterials [24]. Goos–Hänchen shift has been explored by using different kinds of incident beams on different typologies of media. In the literature have been derived the new mathematical expression giving a valuable interpretation of the behavior of the shift in this regard. For example, Airy beams and vortexes when incident on the Dirac metamaterial and graphene-based substrate surfaces are reported [25–28].

Here we have presented the explicit studies for Goos–Hänchen shift while considering both temperature-dependent and temperature-independent absorbing media. Moreover, Drude's model is taken into account in order to dig deep into the temperature-dependent wavelengths, i.e., plasma and damping wavelengths [29]. Moreover, for a better understanding of temperature-dependent reflectivity, contour plots have been reported, Fig. 4.

2. Mathematical model

For the sake of better understanding, we have divided our analysis into two cases, temperature-dependent and temperature-independent GH-shift, and considered both s-polarization and p-polarization in this regard. For the first case, experimental values of the refractive index of metals like silver ($n_{\mathrm{Ag}} = 0.14 + i5.50$), gold ($n_{\mathrm{Au}} = 0.18 + i5.39$), and copper ($n_{\mathrm{Cu}} = 0.260 + i5.26$) have been considered [30]. And for the second case, temperature-dependent refractive index or permittivity has been taken into account for investigating the temperature-dependent Goos–Hänchen shift (GH_T). For this purpose, a famous Drude–Lorentz formulation is used, and we only take gold metal as a second medium due to its chemical stability and extensive usage in modern electronic technology [11].

In this study, a plane incident electromagnetic beam of light (wavelength $\lambda = 826$ nm and its intensity is one volt per meter (1 V/m)) travel from the medium one with refractive index n_1, air in this scenario, to the second medium with complex refractive index $\hat{n_2}$. Both temperature-dependent and temperature-independent cases have been investigated on the same geometry: difference depends upon the second medium's dependency on temperature. Starting from the Fresnel equations, it is possible to find GH-shift through the formulation given by Artmann's stationary phase method [6]. A basic equation for finding the GH-shift is [5,31],

$$D = -\frac{1}{\kappa}\frac{d\delta}{d\theta} \tag{1}$$

$\kappa = \frac{2\pi}{\lambda}$, represents the wave number of the medium, δ and θ show the phase of medium and the angle of incidence, respectively. Reflection coefficients for both s-polarization and p-polarizations are given by [32],

$$R_p = \frac{\hat{n_2}\cos\theta_i - n_1\cos\theta_t}{\hat{n_2}\cos\theta_i + n_1\cos\theta_t} \tag{2}$$

$$R_s = \frac{n_1\cos\theta_i - \hat{n_2}\cos\theta_t}{n_1\cos\theta_i + \hat{n_2}\cos\theta_t} \tag{3}$$

respectively. θ_i is the angle of incidence, while θ_t represents the transmission angle. Studying the optical properties of metals in deep details is not easy: therefore, we assumed Drude's model as a good approximation in this regard [33]. Further, the metal is a complex medium or absorbing medium: therefore, it exhibits the complex permittivity, and Drude's model gives the simple

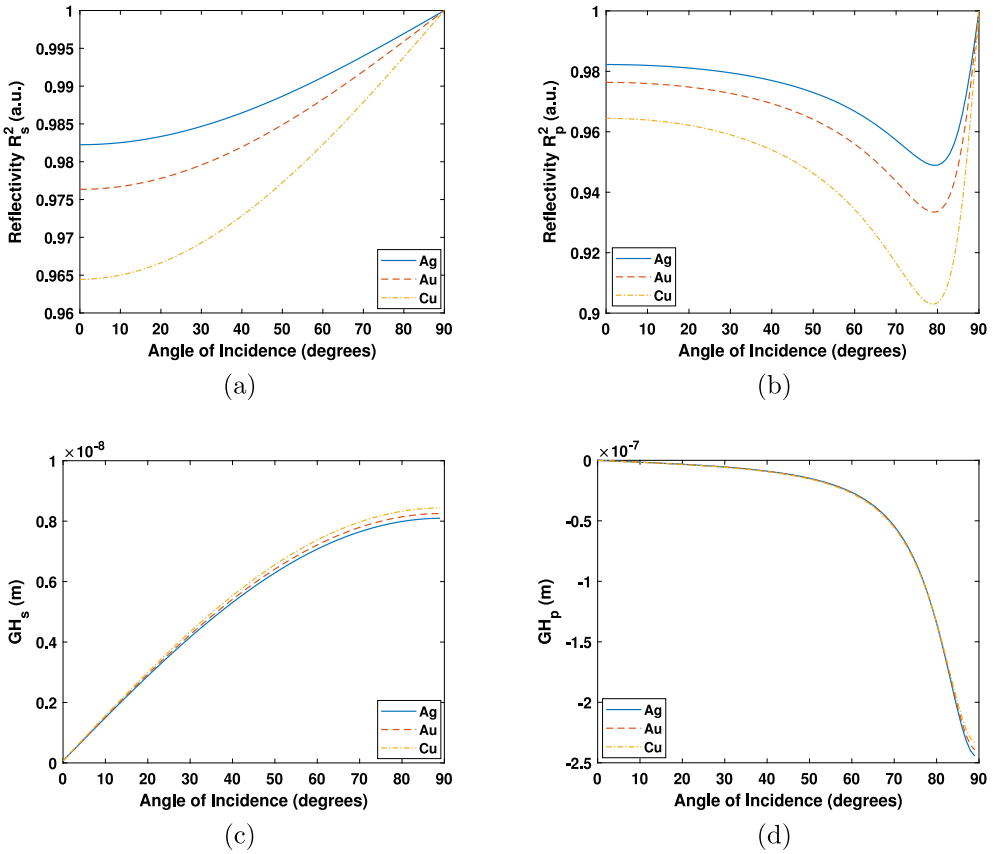

Fig. 2. Behavior of reflectivity $R^2_{s,p}$ and Goos–Hänchen shift $GH_{s,p}$ for the angle of incidence. (a) Behavior of Reflectivity for s-polarized incident beam, (b) Behavior of Reflectivity for a p-polarized incident beam; (c) GH-shift for a s-polarized incident beam; (d) GH-shift for a p-polarized incident beam.

relation for handling the complex permittivity, especially when it depends upon wavelength and temperature [9]. Therefore, Temperature-dependent permittivity as a function of temperature can be given by Drude's model [9],

$$\hat{\epsilon}_2(T) = 1 - \frac{\lambda^2 \lambda_c(T)}{\lambda_p^2(T)(\lambda_c(T) + i\lambda)} \tag{4}$$

In the above relation, λ_p is the plasma frequency, λ_c represents collision, and incident wavelength is denoted by λ. Temperature-dependent plasma wavelength λ_p directly related to the density and effective mass of the electrons, which also depends upon temperature, given by [34],

$$\frac{1}{\lambda_p(T)} = \frac{1}{\lambda_p(T_o)}[1 + 3\gamma_m(T - T_0)]^{(-1/2)} \tag{5}$$

Here $\lambda_p(T_o) = 168.26$ nm represents the plasma wavelength of gold at the room temperature of $T_o = 300$ K. Thermal expansion coefficient of bulk metal is given by $\gamma_m = 1.42 \times 10^{-5}$ K^{-1}. For finding collision wavelength $\lambda_c(T)$, the scattering from both phonon and electron parts must be considered [9].

$$\frac{1}{\lambda_c(T)} = \left[\frac{2\pi c \varepsilon_o}{\lambda^2 \sigma(0)}\right] \frac{\frac{1}{10} + \left(\frac{T}{T_D}\right)^5 \int_0^{T_D/T} \frac{z^4 dz}{(e^z - 1)}}{\int_0^{T_D/T} \frac{z^5 dz}{(e^z - 1)(1 - e^{-z})}} + \frac{\pi^2 \Gamma \Delta}{24 c \hbar E_F} \left[(K_B T)^2 + \left(\frac{\hbar c}{\lambda}\right)^2\right] \tag{6}$$

In Eq. (6), the first term indicates the contribution from phonon–electron scattering and the second term indicates the electron–electron scattering. Further, $\sigma(0) = 7.576 \times 10^7\ \Omega^{-1}\ \text{m}^{-1}$ represents the DC conductivity of gold at Debye temperature of $T_D = 170$ K, and $E_F = 5.53$ eV is the Fermi energy, $\Gamma = 0.55$ represents the average amount of the Fermi surface of the scattering, and $\Delta = 0.77$ represents the umklapp scattering, $\hbar = 1.05457 \times 10^{-34}$ J s is the Plank's constant and $k_B = 1.38062 \times 10^{-23}$ J K^{-1} is the Boltzmann's constant [9,34].

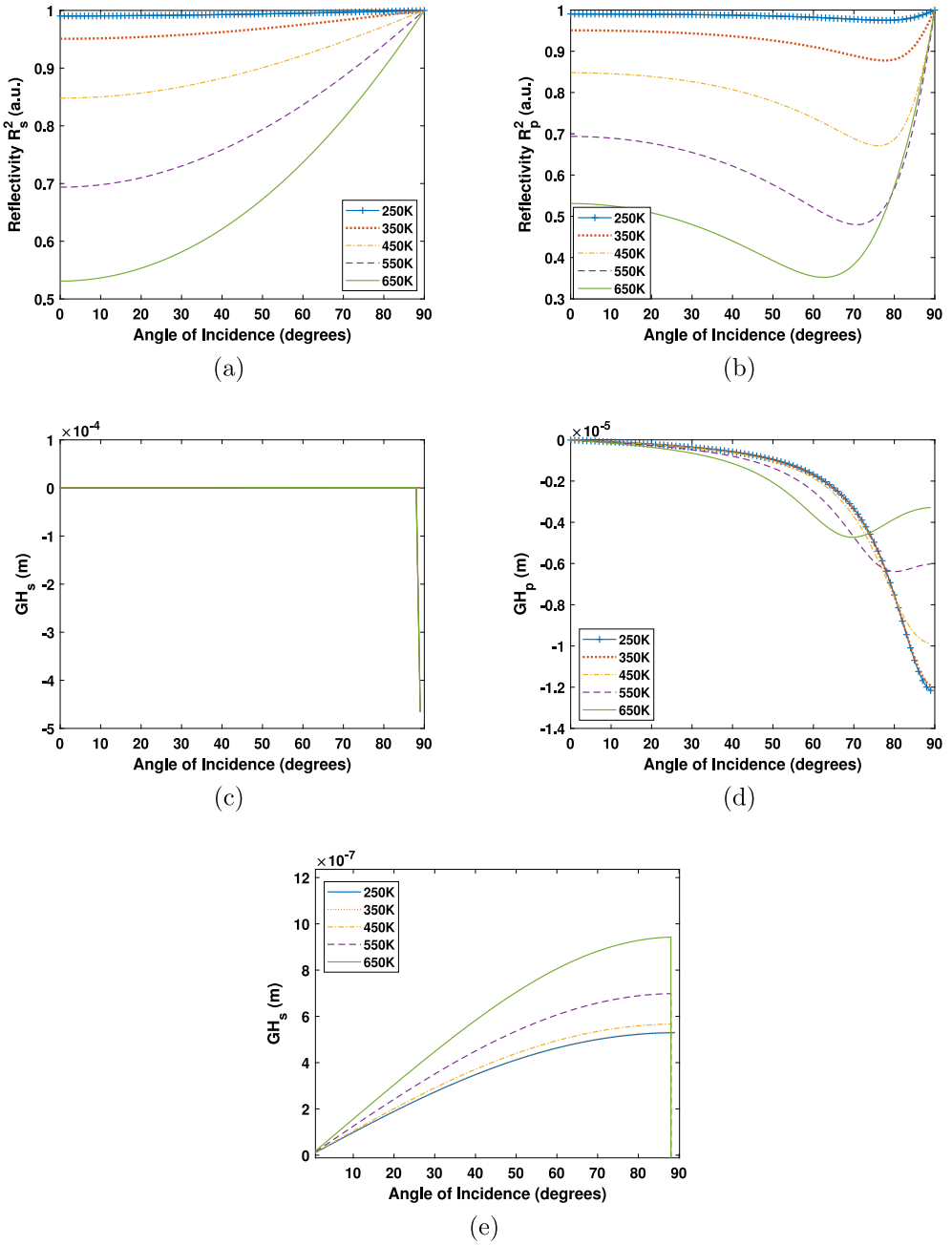

Fig. 3. Behavior of reflectivity $R_{s,p}^2$ and Goos–Hänchen shift $GH_{s,p}$. (a) Behavior of Reflectivity for a *s*-polarized light, (b) Behavior of Reflectivity for a *p*-polarized incident beam, (c) GH-shift for a *s*-polarized incident beam, (d) GH-shift for a *p*-polarized incident beam, (e) Sub-figure (zoom view of Fig. 3(c)) of GH-shift for a *s*-polarized incident beam.

The Phase of reflection coefficient for both *s*-polarization and *p*-polarization is given by [35]

$$\delta_p = Im\left[\ln\left[\frac{\hat{n_2}^2 cos\theta - n_1(\hat{n_2}^2 - n_1^2\sin^2\theta)^{1/2}}{\hat{n_2}^2 cos\theta + n_1(\hat{n_2}^2 - n_1^2\sin^2\theta)^{1/2}}\right]\right] \tag{7}$$

$$\delta_s = Im\left[\ln\left[\frac{n_1 cos\theta - (\hat{n_2}^2 - n_1^2\sin^2\theta)^{1/2}}{n_1 cos\theta + (\hat{n_2}^2 - n_1^2\sin^2\theta)^{1/2}}\right]\right] \tag{8}$$

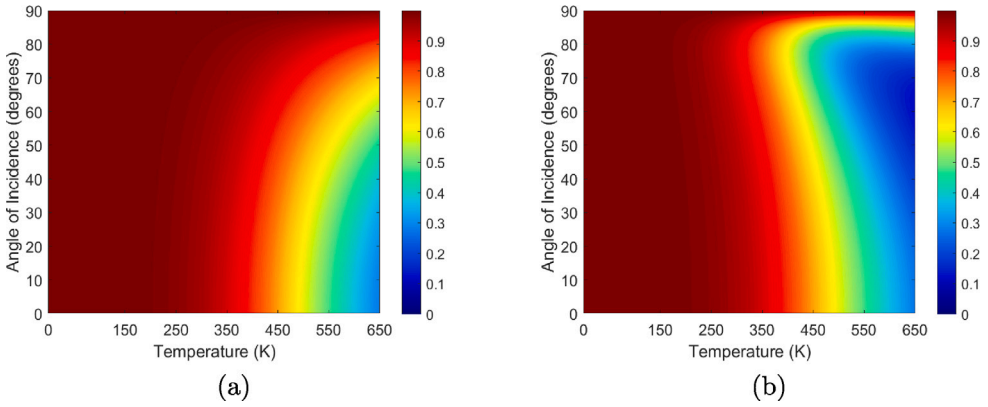

Fig. 4. Contour plots of reflectivity as a function of temperature, incident angle (vertical axes), temperature (horizontal axes), and color bar indicates the reflectivity from 0.2 (blue) to 0.9 (red), (a) Reflectivity when the incident field is *s*-polarized, (b) Reflectivity when the incident field is *p*-polarized. (For interpretation of the references to color in this figure legend, the reader is referred to the web version of this article.)

As the dielectric constant or refractive indices are complex in our case for the second medium and can be inter-convertible by using the following relation [36],

$$\hat{n} = n + i\kappa$$
$$\hat{\epsilon} = \epsilon_r + \epsilon_i = \hat{n}^2$$
$$\hat{n}(T) = \sqrt{\hat{\epsilon}(T)}$$

3. Results and discussion

The basic idea behind this study is to explore the Goos–Hänchen shift when it depends upon temperature-dependent complex dielectric constant and to explore the factors which contribute to makeing temperature-dependent Goos–Hänchen shift different from simple temperature-independent shift. For the temperature-independent GH-shift values of dielectric constant are fixed and do not depend upon temperature, results for reflectivity and Goos–Hänchen shift are shown in Fig. 2. For the temperature-dependent GH-shift we have used temperature-dependent permittivity or complex dielectric constant as a function of temperature for a gold only, results for reflectivity and GH-shift can be seen in Fig. 3.

In Figs. 2(a) and 3(a), it can be seen that the reflectivity R_s^2 increases with the increase in the angle of incidence for *s*-polarization in both cases of temperature-independent and temperature-dependent permittivity, respectively. And maximum reflection has been occurred at 90° for all the values of temperature. For *p*-polarization, in Figs. 2(b) and 3(b), decreasing behavior of reflectivity R_p^2 can be seen with respect to the angle of incidence; however, this trend starts to increase after a specific value of the angle of incidence has been reached. In Fig. 3(b), due to temperature dependency, reflectivity is decreases with the temperature (250 K to 650 K) while the angle of incidence shifts towards bigger values due to temperature-dependent parameter.

Figs. 2(c) and 3(c, e) represent the positive GH-shift for *s*-polarization, in both scenarios (temperature-independent case and temperature-dependent case) of Goos–Hänchen. Fig. 3(e) shows a more detailed view of Fig. 3(c). For *p*-polarization, negative Goos–Hänchen shifts are observed in Figs. 3(d) and 4(d). In Fig. 3(d), GH-shift shows the same trend for all three metals and its value is decreasing and has a minimum value at 90°, while in Fig. 4(d), it can be seen that for temperature-dependent Goos–Hänchen shift at lower temperatures (250 K and 350 K) it shows almost similar behavior just like in temperature-independent case, but as the temperature rises after 350 K, shift displays its deviating behavior at the specific values of angle of incidence, i.e., drops at certain angles and then starts to rise again. In addition, the maximum rise of this shift can be seen for the maximum temperature (650 K). Finally, in Fig. 4(a,b), contour plots of reflectivity (for both *s* and *p*-polarization) as a function of temperature have been shown for the better understanding of the concept of the temperature dependency on reflectivity and the angle of incidence. In this Figure, vertical axes display incident angle and horizontal axes show the rise in the temperature and color-bar indicates the reflectivity from blue to red area.

4. Conclusion

In this work, we have seen how temperature-dependent refractive index or permittivity and angle of incidence impact the reflectivity and Goos–Hänchen shift. For both polarization (*s* and *p*), reflectivity is inversely related to the temperature, i.e., an increase in reflectivity gives a decrease in the values of temperature. Moreover, GH-shifts are positive and negative for *s* and *p* polarization. This study may be helpful to develop a temperature-sensitive devices based on this shift. This shift parameter can be effectively used to control the temperature according to the requirements.

Declaration of competing interest

The authors declare that they have no known competing financial interests or personal relationships that could have appeared to influence the work reported in this paper.

Data availability

Data will be made available on request.

References

[1] F. Mangini, F. Frezza, Analysis of the electromagnetic reflection and transmission through a stratified lossy medium of an elliptically polarized plane wave, Math. Mech. Complex Syst. 4 (2) (2016) 153–167.
[2] F. Mangini, F. Frezza, On zero-reflection and zero-transmission of a stratified lossy medium, in: Proceeding URSI International Symposium on Electromagnetic Theory, EMTS, 2016, pp. 755–758.
[3] S.J. Orfanidis, Electromagnetic waves and antennas, Vol. 1, Rutgers University, 2016.
[4] F. Goos, H. Hänchen, Ein neuer und fundamentaler versuch zur totalreflexion, Ann. Phys. 436 (7–8) (1947) 333–346.
[5] A. Mehboob, A.A. Syed, Q.A. Naqvi, Studying the Goos–Hänchen shift in the presence of non-integer dimensional space, Optik 181 (2019) 1066–1074.
[6] K. Artmann, Calculation of the lateral shift of totally reflected beams, Ann. Physics 437 (1948) 87–102.
[7] M. Merano, A. Aiello, M. Van Exter, J. Woerdman, Observing angular deviations in the specular reflection of a light beam, Nat. Photonics 3 (6) (2009) 337–340.
[8] M. Shah, Electrically tunable Goos–Hänchen shift in two-dimensional quantum materials, Opt. Mater. Express 12 (2) (2022) 421–435.
[9] Y. Xu, L. Wu, L.K. Ang, Ultrasensitive optical temperature transducers based on surface plasmon resonance enhanced composited Goos–Hänchen and Imbert-Fedorov shifts, IEEE J. Sel. Top. Quantum Electron. 27 (6) (2021) 1–8.
[10] X. Yin, L. Hesselink, Goos–Hänchen shift surface plasmon resonance sensor, Appl. Phys. Lett. 89 (26) (2006) 261108.
[11] Y. Wang, H. Li, Z. Cao, T. Yu, Q. Shen, Y. He, Oscillating wave sensor based on the Goos–Hänchen shift effect, Appl. Phys. Lett. 92 (6) (2008) 061117.
[12] F. Bretenaker, A. Le Floch, L. Dutriaux, Direct measurement of the optical Goos–Hänchen effect in lasers, Phys. Rev. Lett. 68 (7) (1992) 931.
[13] R.H. Renard, Total reflection: a new evaluation of the Goos–Hänchen shift, JOSA 54 (10) (1964) 1190–1197.
[14] P. Leung, C. Chen, H. Chiang, Large negative Goos–Hänchen shift at metal surfaces, Opt. Commun. 276 (2) (2007) 206–208.
[15] A. Lakhtakia, On planewave remittances and Goos–Hänchen shift of planar slabs with negative real permittivity and permeability, Electromagnetics 23 (1) (2003) 71–75.
[16] M. Merano, A. Aiello, M. Van Exter, E. Eliel, J. Woerdman, et al., Observation of Goos–Hänchen shift in metallic reflection, Opt. Express 15 (24) (2007) 15928–15934.
[17] O.J. Santana, L.E. de Araujo, Direct measurement of the composite Goos–Hänchen shift of an optical beam, Opt. Lett. 43 (16) (2018) 4037–4040.
[18] N.I. Petrov, V.A. Danilov, V.V. Popov, B.A. Usievich, Large positive and negative Goos-Hänchen shifts near the surface plasmon resonance in subwavelength grating, Opt. Express 28 (5) (2020) 7552–7564.
[19] N.I. Petrov, Y.M. Sokolov, V.V. Stoiakin, V.A. Danilov, V.V. Popov, B.A. Usievich, Observation of giant angular Goos-Hanchen shifts enhanced by surface plasmon resonance in subwavelength grating, in: Photonics, Vol. 10, MDPI, 2023, p. 180.
[20] C.W. Chen, W.C. Lin, L.S. Liao, Z.H. Lin, H.P. Chiang, P.T. Leung, E. Sijercic, W.S. Tse, Optical temperature sensing based on the Goos–Hänchen effect, Appl. Opt. 46 (22) (2007) 5347–5351.
[21] W.I. Waseer, Q.A. Naqvi, M.J. Mughal, Analysis of the Goos–Hänchen shift for a planar interface of NID dielectric and general medium, Optik 218 (2020) 165140.
[22] M. Zoghi, Goos–Hänchen and Imbert–Fedorov shifts in a two-dimensional array of gold nanoparticles, J. Nanophotonics 12 (1) (2018) 016021.
[23] W.J. Wild, C.L. Giles, Goos-Hänchen shifts from absorbing media, Phys. Rev. A 25 (4) (1982) 2099.
[24] Y.-q. Kang, Y. Xiang, C. Luo, Tunable enhanced Goos–Hänchen shift of light beam reflected from graphene-based hyperbolic metamaterials, Appl. Phys. B 124 (6) (2018) 1–6.
[25] Q. Yue, X. Zhou, D. Deng, Goos–Hänchen and Imbert-Fedorov shifts of the airy beam in Dirac metamaterials, New J. Phys. (2023).
[26] W. Zhen, D. Deng, Goos–Hänchen shifts for airy beams impinging on graphene-substrate surfaces, Opt. Express 28 (16) (2020) 24104–24114.
[27] M. Gao, D. Deng, Spatial Goos–Hänchen and Imbert-Fedorov shifts of rotational 2-D finite energy airy beams, Opt. Express 28 (7) (2020) 10531–10541.
[28] M. Gao, G. Wang, X. Yang, H. Liu, D. Deng, Goos–Hänchen and Imbert-Fedorov shifts of off-axis airy vortex beams, Opt. Express 28 (20) (2020) 28916–28923.
[29] H.-P. Chiang, P. Leung, W.-S. Tse, Optical properties of composite materials at high temperatures, Solid State Commun. 101 (1) (1997) 45–50.
[30] D.P. Edward, I. Palik, Handbook of optical constants of solids, 1985.
[31] A. Mehboob, A.A. Syed, Q.A. Naqvi, Investigating the Goos-Hänchen shift for a fractional dual planar interface, Optik 185 (2019) 910–916.
[32] C. Balanis, Advanced Engineering Electromagnetics, Wiley, 2012.
[33] K. Ujihara, Reflectivity of metals at high temperatures, J. Appl. Phys. 43 (5) (1972) 2376–2383.
[34] A.K. Sharma, H.S. Pattanaik, G.J. Mohr, On the temperature sensing capability of a fibre optic SPR mechanism based on bimetallic alloy nanoparticles, J. Phys. D: Appl. Phys. 42 (4) (2009) 045104.
[35] A. Mehboob, F. Mangini, F. Frezza, Exploring the temperature-dependent Goos-Hänchen shift on a metal surface, in: 2022 IEEE 21st Mediterranean Electrotechnical Conference, MELECON, IEEE, 2022, pp. 285–289.
[36] G. Turhan-Sayan, et al., Temperature effects on surface plasmon resonance: design considerations for an optical temperature sensor, J. Lightwave Technol. 21 (3) (2003) 805.